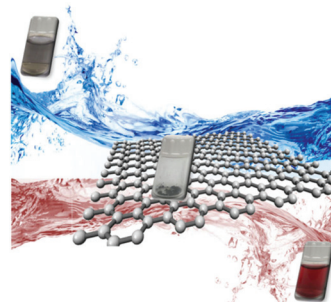


1

Production and stability of mechanochemically exfoliated graphene in water and culture media

V. León, J. M. González-Domínguez, J. L. G. Fierro, M. Prato and E. Vázquez*

To prepare graphene in water is a highly desired goal for biological and medicinal studies. Here we show that freeze-dried graphene powders prepared by ball milling treatments may be easily reverted to aqueous suspensions, including in cell culture media, without damaging its structure. Such a step forward uncovers the potential benefits (and drawbacks) that should be paid attention to.



Q3

Please check this proof carefully. **Our staff will not read it in detail after you have returned it.**

Translation errors between word-processor files and typesetting systems can occur so the whole proof needs to be read. Please pay particular attention to: tabulated material; equations; numerical data; figures and graphics; and references. If you have not already indicated the corresponding author(s) please mark their name(s) with an asterisk. Please e-mail a list of corrections or the PDF with electronic notes attached – do not change the text within the PDF file or send a revised manuscript. Corrections at this stage should be minor and not involve extensive changes. All corrections must be sent at the same time.

Please bear in mind that minor layout improvements, e.g. in line breaking, table widths and graphic placement, are routinely applied to the final version.

We will publish articles on the web as soon as possible after receiving your corrections; **no late corrections will be made.**

Please return your **final** corrections, where possible within **48 hours** of receipt, by e-mail to: nanoscale@rsc.org

Queries for the attention of the authors

Journal: **Nanoscale**

Paper: **c6nr03246j**

Title: **Production and stability of mechanochemically exfoliated graphene in water and culture media**

Editor's queries are marked like this [Q1, Q2, ...], and for your convenience line numbers are indicated like this [5, 10, 15, ...].

Please ensure that all queries are answered when returning your proof corrections so that publication of your article is not delayed.

Query Reference	Query	Remarks
Q1	For your information: You can cite this article before you receive notification of the page numbers by using the following format: (authors), Nanoscale, (year), DOI: 10.1039/c6nr03246j.	
Q2	Please carefully check the spelling of all author names. This is important for the correct indexing and future citation of your article. No late corrections can be made.	
Q3	Please check that the Graphical Abstract text fits within the allocated space indicated on the front page of the proof. If the entry does not fit between the two horizontal lines, then please trim the text and/or the title.	
Q4	The sentence beginning "As commonly accepted..." has been altered for clarity, please check that the meaning is correct.	
Q5	In the sentence beginning "A very recent example has..." should "sonication pressure" be changed to "sonication frequency"?	
Q6	The sentence beginning "From the %N..." has been altered for clarity, please check that the meaning is correct.	
Q7	The citation to Fig. 1d and e in the sentence beginning "For re-suspended BMG..." has been changed to Fig. 3d and e as the text appears to discuss Fig. 3d and e. Please check that this is correct.	
Q8	The meaning of the sentence beginning "This striking outcome..." is not clear - please provide alternative text.	

Production and stability of mechanochemically exfoliated graphene in water and culture media†

V. León,^{‡a} J. M. González-Domínguez,^{‡a} J. L. G. Fierro,^b M. Prato^{c,d,e} and E. Vázquez^{*a}

Cite this: DOI: 10.1039/c6nr03246j

Received 20th April 2016,
Accepted 27th June 2016
DOI: 10.1039/c6nr03246j

www.rsc.org/nanoscale

The preparation of graphene suspensions in water, without detergents or any other additives is achieved using freeze-dried graphene powders, produced by mechanochemical exfoliation of graphite. These powders of graphene can be safely stored or shipped, and promptly dissolved in aqueous media. The suspensions are relatively stable in terms of time, with a maximum loss of ~25% of the initial concentration at 2 h. This work provides an easy and general access to aqueous graphene suspensions of chemically non-modified graphene samples, an otherwise (almost) impossible task to achieve by other means. A detailed study of the stability of the relative dispersions is also reported.

Introduction

The recent excitement on graphene (GR) research has driven a continuous flow of work, directed towards the common goal of unravelling the properties of this new material, in order to exploit its potential technological outputs.^{1,2} As commonly accepted, reliable mass production and processing of GR is still a bottleneck for interesting applications (such as filler in composite materials, drug delivery vectors, or as analytical platforms), though many promising methods have been identified.³ High quality monolayer graphene can be obtained by epitaxial growth or chemical vapor deposition methods, so that the as-obtained materials can be applied to high-performance optoelectronics.³ However, other fields, such as nanocomposites or nanomedicine, require bulk quantities of graphene, not feasible through a scale-up of the above mentioned synthetic methods.¹ Initial interesting efforts in these latter fields have been addressed by using chemical derivatives

of GR (namely its oxide, GO, and its reduced counterpart RGO), but the results are far from being transferable to pristine GR. Perhaps, the most reliable way to obtain a suitable unmodified GR material, cost-efficiently, and in the desired amounts is the exfoliation of graphite.^{4–6} The progress in making stable dispersions of GR allows the production of few-layer GR materials with several hundred nm in flake size, some basal plane defects and oxygen functionalities but with large areas of undamaged structure, hence good structural characteristics to enable their exploitation, for example, in composite applications. However, toxicological, bioimaging or biomedical studies (*in vitro* and *in vivo*) of GR have so far mainly focused on GO and RGO,^{7,8} with very little research on pristine GR. The main reason for this gap is the difficulty to obtain pristine GR flakes directly in water or in culture media. A very recent example has shown how to exfoliate graphite in pure water by adjusting the sonication pressure and temperature and the GR storage conditions (0.0065 mg mL⁻¹),⁹ but regardless, the most common approach is to help the exfoliation in water using additives. Some studies have pursued this by exfoliation of graphite in aqueous media with, for example, pyrene derivatives,^{10–12} anionic surfactants,^{13,14} polymers,^{15,16} or proteins.^{15–18}

Therefore, whereas GO powders can be directly dispersed in the cell culture medium (CCM) or transferred through dilution with water,⁸ pristine (chemically non-modified) GR in aqueous suspension is mostly handled with its accompanying dispersant,^{15,17} or (hardly ever reported) GR powders directly dispersed in CCM.¹⁹ However, these latter authors found adsorptive artifacts due to the large surface area of GR, which cause non-covalent interactions with the CCM components.

Despite the increasing interest in the use of GR in biological applications, another factor that seems to be partly ignored

^aOrganic and Inorganic Chemistry and Biochemistry Department, University of Castilla-La Mancha, Avda. Camilo José Cela S/N, 13071 Ciudad Real, Spain.

E-mail: ester.vazquez@uclm.es

^bInstituto de Catálisis y Petroquímica (ICP-CSIC), Marie Curie, 2, Cantoblanco, 28049 Madrid, Spain

^cDepartment of Chemical and Pharmaceutical Sciences, University of Trieste, Piazzale Europa 1, 34127 Trieste, Italy

^dCarbon Nanobiotechnology Laboratory, CIC biomaGUNE, Paseo de Miramón 182, 20009 Donostia-San Sebastian, Spain

^eIkerbasque, Basque Foundation for Science, E-48011 Bilbao, Spain

†Electronic supplementary information (ESI) available: A video showing the dispersion process, the N 1s XPS spectrum of BMG, image of the graphite test in CCM, and the characterization of the GO employed. See DOI: 10.1039/c6nr03246j

‡These authors contributed equally to this work.

relates to the colloidal properties of GR materials in biological media. CCM could selectively stabilize materials with particular physicochemical properties, while, on the other hand, aggregation (irreversible inter-laminar adherence) may produce misleading results, hindering experimental reproducibility and indirectly influencing the cellular response. Moreover, macromolecular dispersants (polymers, proteins), which are not easily quantifiable, may play a non-negligible role at a cellular level. As a general comment, we can assert that there is still a lot to elucidate on the use of pristine GR for biological applications.

Recently, we have reported a facile and inexpensive ball milling process to exfoliate graphite.^{20,21} Stable graphene suspensions in polar solvents, including water, have been prepared paving the way towards hydrogel nanocomposites²² or film casting for cellular interaction studies.²³ In the present work, we have tackled the processing of GR samples in such a way that GR can be easily handled and transferred to any liquid medium, preserving its original features, with the aim of empowering the studies in the biomedical field. Also, the stability of the relative suspensions in water and CCM has been studied in detail.

Results and discussion

The synthesis of aqueous suspensions of GR can be achieved using a ball milling technique (ball-milled graphene, BMG), with melamine (2,4,6-triaminotriazine) as the only adjuvant (see the Experimental section). Melamine is ideally suited as an exfoliating agent, because it forms extended π -systems through multiple H-bonds.^{20,21} Melamine gets inserted among the layers of graphite, leading to mono- and few-layer graphene, eventually stabilized in liquid media.²¹ Since melamine is considered toxic,^{§²⁴} we made considerable efforts to efficiently remove most of the melamine, without altering the GR colloidal stability. This was achieved by simply washing the sample with hot water, and controlling the melamine content in the graphene samples through elemental analysis (EA), which resulted in less than 1 ppm in water suspensions of $\sim 0.1 \text{ mg mL}^{-1}$ of freshly produced BMG. These aqueous suspensions of GR samples were rapidly frozen and, subsequently, lyophilized in a freeze-drier giving rise to a very soft and low-density black powder (Fig. 1), essentially made of few-layer GR sheets as its parent suspension. The mass yield of the process was $\sim 30\%$.

The characterization of the powder was conducted by means of thermogravimetric analysis (TGA), X-ray photoelectron spectroscopy (XPS) and EA. The latter gave average values of: C ($94.3 \pm 0.2 \text{ wt\%}$), H ($0.42 \pm 0.02 \text{ wt\%}$) and N ($0.36 \pm 0.01 \text{ wt\%}$), with the amount of oxygen less than 5 wt%, in agreement with the 7 wt% loss observed by TGA in Fig. 2a. From the %N obtained from EA we estimate that the content

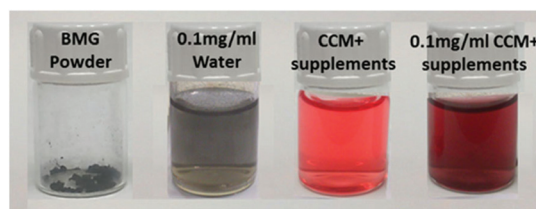


Fig. 1 Photographs of BMG powder and its dispersions in water and CCM + supplements (10% FBS and 1% Gentamycin sulfate).

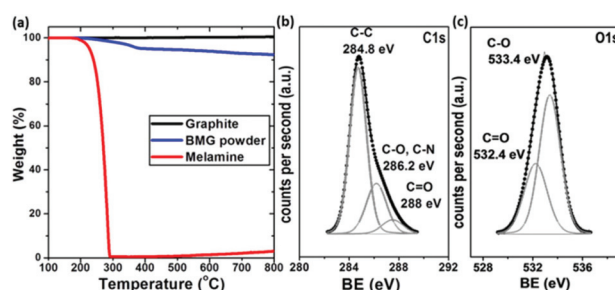


Fig. 2 (a) TGA plots of graphite, BMG powder and melamine; (b) C 1s XPS of BMG powder; (c) O 1s XPS of BMG powder.

of melamine within the BMG powder is $0.54 \pm 0.01 \text{ wt\%}$. XPS deconvoluted plots (Fig. 2b and c) confirmed the presence of some oxygen groups, from the C 1s and O 1s core level spectra and traces of melamine (Fig. S1, ESI[†]). We bath-sonicated the BMG powders in ultrapure water (at various concentrations) using mild pulses combined with shaking, until a fine dark suspension was obtained (see video in the ESI[†]). The powder could be re-dispersed in water at the desired concentration (Fig. 1), generating concentrated BMG suspensions (up to a maximum of 0.3 mg mL^{-1}), which can be further diluted to match the desired concentration. To check whether the re-dispersed BMG keeps its structural integrity after going through the whole drying and re-dispersing process, we carried out an extensive Raman spectroscopy study. In Fig. 3a representative Raman spectra are reported, where the GR characteristic bands, the tangential (G), the disordered (D) and its second order (2D) modes are clearly visible. By recording different spectra at random locations of each BMG sample, we probed these bands in the re-dispersed powder. As displayed in Fig. 3b and c the full-width at half maximum (FWHM) of the G and 2D bands does not depend on their respective positions in different Raman spectra (Pos(G) and Pos(2D)), as reported for single-layer GR, which was taken as a first proof of GR integrity.²⁵

Comparing two different sonication times in water (*i.e.*, 1 and 15 min, Fig. 4), it is evident that higher sonication times led to somewhat lower values of the FWHM(2D) in the statistical distribution, with no significant variation in its position. Since narrow 2D bands have usually been reported for a small number of layers,^{26,27} a reasonable and simple explanation of the above result would be a more efficient re-dispersion of GR

§ According to the World Health Organization, the melamine limit to consider contamination of a food sample ranges between 1 and 2.5 ppm. See ref. 24.

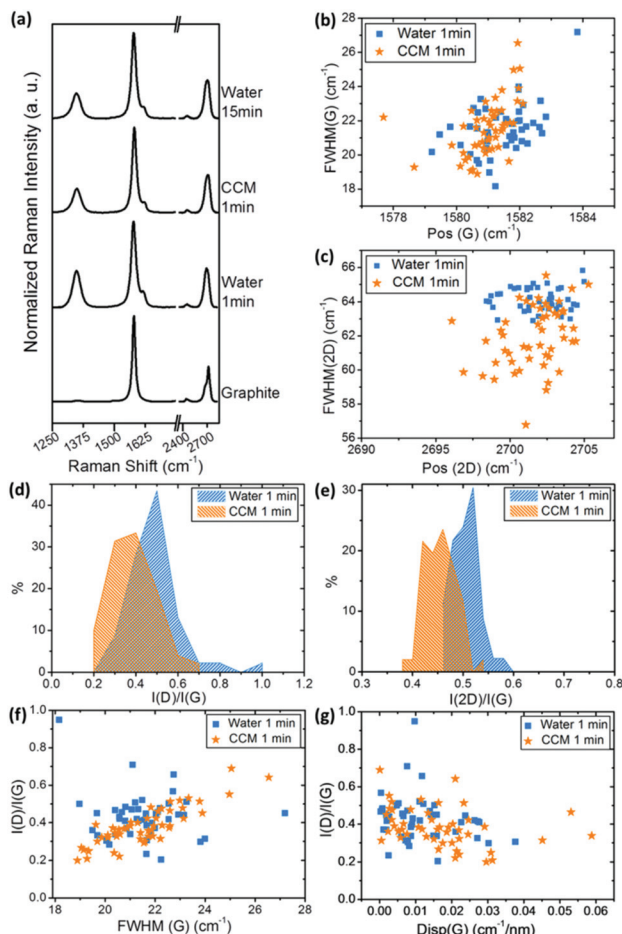


Fig. 3 (a) Comparison of Raman spectra of graphite, re-dispersed BMG powder in water and CCM at 532 nm; (b) FWHM(G) vs. Pos(G); (c) FWHM(2D) vs. Pos(2D) recorded at different locations of the sample; (d) distribution of $I(D)/I(G)$ and (e) $I(2D)/I(G)$; (f) $I(D)/I(G)$ as a function of FWHM(G) at 532 nm; (g) Disp(G) for BMG powder.

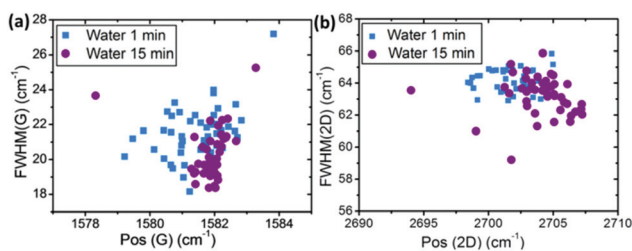


Fig. 4 (a) FWHM(G) versus Pos(G) and (b) FWHM(2D) versus Pos(2D) recorded on different locations of the sample with a 532 nm laser wavelength.

flakes, simply due to longer sonication times, which would imply the higher exposure of GR powders to the sonication-induced cavitation effect.⁴ In addition, the level of defects was checked by analyzing the $I(D)/I(G)$ ratio (Fig. 3d).²⁸ The results show that 15 min of ultrasonication does not induce more defects in the GR structure and a rise and slight narrowing of

the 2D band is prevalent (Fig. 3a). For re-suspended BMG in water at 1 min sonication time, $I(D)/I(G)$ ranges between 0.2 and 0.6, whilst $I(2D)/I(G)$ ranges between 0.45 and 0.6 (Fig. 3d and e). This confirms that the sample is a few-layer GR, usually assigned for $I(2D)/I(G) < 1$,²⁶ while the numbers observed are in accordance with the original BMG.^{20–23} Moreover, reproducible two-dimensional Raman mappings, applied to larger sections of the sample (Fig. 5), point to a homogeneous composition and ultimately confirm the successful resuspension of BMG powder in an aqueous solution with no change in its structure.

The BMG powder was also successfully dispersed in CCM. Fig. 3a–e display Raman features of GR arising from CCM dispersion, compared to those in water. Pos(G) and FWHM(G) do not vary significantly from that of water (Fig. 3b), but FWHM(2D) statistically reaches much lower values in CCM (Fig. 3c). This narrowing of the 2D band might again be ascribed to the higher exfoliation efficiency of CCM in just 1 min of sonication, providing even better results with respect to water after 15 min of ultrasonication (Fig. 4), possibly due to the dispersant effect of the CCM components. From $I(D)/I(G)$ it seems that the level of defects (Fig. 1d) is slightly lower in the case of CCM. Presumably, the effects of ultrasound could be damped by the CCM components, or also, the higher exfoliation achieved in CCM provides more available surface with non-damaged basal planes, lowering in average the amount of defects. It should be added that an identical methodology was followed for pristine graphite powders (sonication for 1 and 15 min in CCM) and no appreciable degree of dispersion or exfoliation was noticed (representative images in Fig. S2, ESI†).

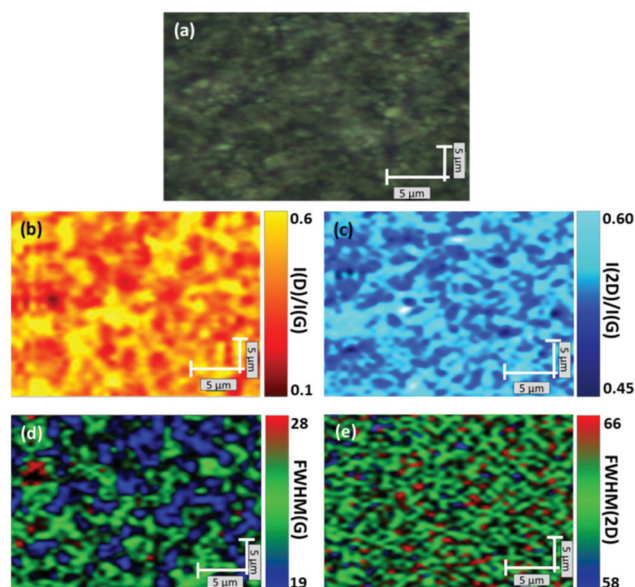


Fig. 5 (a) Optical microscopy image of BMG powder after re-dispersion in water. Two-dimensional Raman mappings of (b) $I(D)/I(G)$ and (c) $I(2D)/I(G)$, (d) FWHM(G) and (e) FWHM(2D) of BMG powder re-dispersed in water at 532 nm. Note that mappings displayed in (b–e) correspond to the same sample area shown in (a).

A further analysis of the defects led to the graphics displayed in Fig. 3f and g. It has been reported that the dependence of $I(D)/I(G)$ with $\text{FWHM}(G)$ or with the G peak dispersion ($\text{Disp}(G)$)[¶] allows to discriminate between disordered carbon at the edges or at the basal plane in GR samples.²⁸ As observed for the re-suspended BMG in water, there is no correlation between $I(D)/I(G)$ and $\text{FWHM}(G)$ or $\text{Disp}(G)$,^{||} which is an indication that the defects are mostly localized at the edges of the BMG flakes.^{23,28} For CCM-suspended BMG, there is a slight linear dependence of $I(D)/I(G)$ with $\text{FWHM}(G)$,^{||} which, according to the literature, points to disordered carbon in the bulk of GR flakes.²⁸ However, we have previously observed that $I(D)/I(G)$ values in CCM are lower than those in water (Fig. 3d), so we assume that no new defects have been created. Moreover, the overall $\text{Disp}(G)$ values are mostly comprised within $0.03 \text{ cm}^{-1} \text{ nm}^{-1}$, far below $0.1 \text{ cm}^{-1} \text{ nm}^{-1}$, above which disordered carbons appear.^{29,30} By taking into account such findings, we postulate that the dependence of $I(D)/I(G)$ with $\text{FWHM}(G)$ in CCM, without evidence of new induced defects, might be ascribed to an effect of the CCM itself.

TEM images of the different re-suspended BMG samples are shown in Fig. 6a–d. As can be observed, there are no noticeable differences among flake morphologies between water and CCM. Both samples display the same shape and wrinkly aspect as the original BMG suspensions.^{20,21} By performing a statistical analysis of these images we obtained average lateral dimensions of $626 \pm 390 \text{ nm}$ for BMG in water (Fig. 6e). We can distinguish between a major population $<1 \mu\text{m}$ and a minor population of $1\text{--}2 \mu\text{m}$, this major population being approximately two thirds of the whole distribution. In the case of BMG in CCM, the majority of sheets have a lateral dimension average of $389 \pm 243 \text{ nm}$ (Fig. 6f), and this result, together with Raman data, suggests that CCM is able to disperse smaller flakes with a less number of graphene layers. This aspect requires additional and more detailed studies, including cryo-TEM experiments.

Despite the increasing use of GR materials in biomedical applications, the possible changes in the colloidal properties of GR in biological media have been hardly discussed. The experimental evaluation of the colloidal stability in CCM is a challenging task and can be addressed by using different techniques.³¹ We have checked the colloidal stability in time by using UV-Vis absorption spectroscopy. We took the Abs values at 660 nm to determine the concentration of the re-suspended BMG in water or CCM over time, and the results are shown in Fig. 7b–e. When re-dispersing BMG in water at various initial concentrations (Fig. 7a) a partial sedimentation of GR over time can be observed. This process is markedly faster in the first few minutes and tends to become stationary after the first

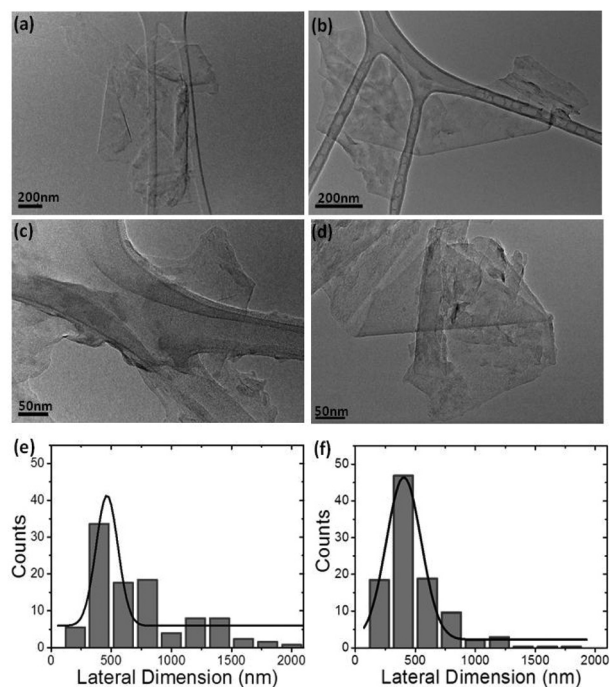


Fig. 6 (a, c) Representative TEM images of re-dispersed BMG powder in water and (b, d) in CCM. Statistical lateral dimension Gaussian distribution from TEM images of BMG powder in (e) water and (f) CCM.

couple of hours. Even though higher initial concentrations seem to lead to larger amounts of sediments, we have observed that this change is always in the range of 25–30% of the initial BMG concentration.

When focusing on CCM, a highly recommended step before proceeding to disperse GR is the pre-dispersion of GR derivatives in serum (such as fetal bovine serum, FBS), whose proteins are able to cover the GR surface, hence improving long-term colloidal stability and mitigating cytotoxicity.^{19,32} For this reason, in many occasions, CCM is supplemented with FBS and antibiotics, because of the requirements of particular biological experiments,⁸ so that the action of exogenous components in CCM should also be taken into account. For this reason, we decided to analyze the GR colloidal stability in both media (CCM with and without supplements, namely FBS and an antibiotic). A comparison between CCM with and without additives (Fig. 1 and 7b) shows that there is only a slight improvement when using additives, particularly in the first hour of sedimentation. Since some biological assays will need such supplements and others will not, this finding will prove useful towards the use of GR powder in any situation. Since there are no significant differences, we continued the stability study in supplemented CCM, which is the most useful medium for biological studies. The study of BMG re-dispersion at different concentrations (Fig. 7c) revealed a stabilization process entailing 20–35% loss of the initial concentration after 2 h. Surprisingly, there is a similar behavior to that of water: a sedimentation profile independent of the initial concentration, with very similar ratios. Finally, the stability over

[¶] $\text{Disp}(G)$ is defined as $\Delta\text{Pos}(G)/(\lambda_1 - \lambda_2)$, where the difference in the G peak position ($\text{Pos}(G)$) taken with two different lasers is divided by the difference in wavelength of such lasers (λ). See ref. 27.

^{||} A linear fitting on both distributions in Fig. 3f revealed a correlation factor (R^2) of 0.03 for water and 0.7 for CCM.

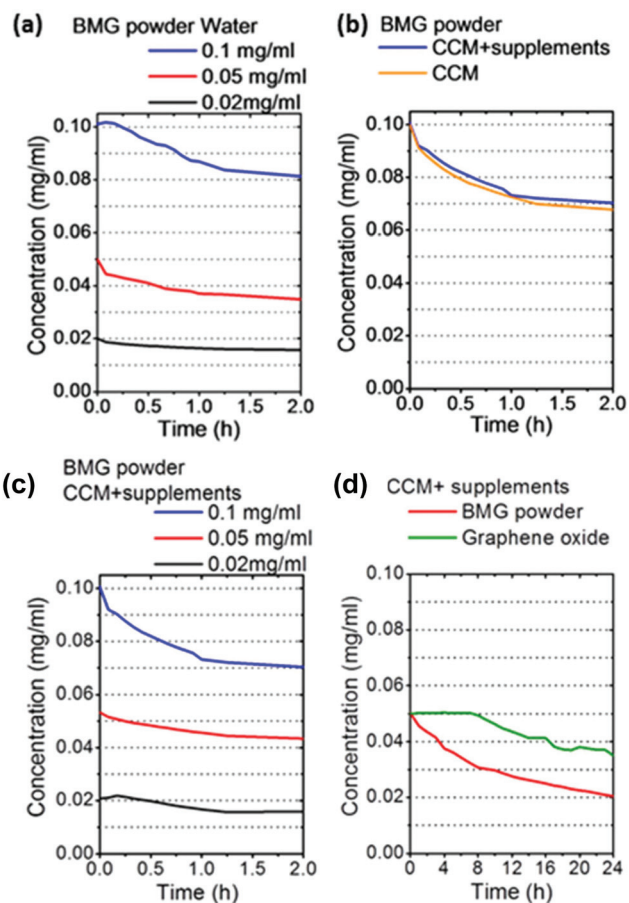


Fig. 7 UV-Vis concentration monitoring: (a) re-dispersed BMG powder in water at different initial concentrations; (b) comparison of re-dispersed BMG powders in as-obtained and supplemented CCM; (c) re-dispersed BMG in supplemented CCM at different initial concentrations; (d) re-dispersed BMG powders and GO in supplemented CCM. Note that supplemented CCM is denoted as 'CCM + supplements' and actually corresponds to the addition of 10% FBS and 1% Gentamycin sulfate to CCM.

longer periods of time is shown in Fig. 7d, where BMG sediments at a faster rate up to the first 8 h and much slower thereafter.

As a first approach for analyzing the material that remains in solution we have studied the GR dispersions in water after 2 and 24 h of settlement by TEM (Fig. 8). The TEM images exhibit in both cases a major population <1 μm which gathers ~97% of the size distribution. After 2 h many large flakes had deposited (as compared to the freshly prepared, Fig. 6e) but a small fraction above 1 μm is still present (corresponding to the remaining ~3%). This tiny population of large flakes eventually disappears after 24 h, leaving only the smaller flakes in suspension. This striking outcome arises a critical point about the characteristics of suspended GR over time, by which the initial system evolves in 2 h to different features, and so forth after 24 h.

Q8

Finally, all these results were compared to those of a commercial GO sample, which presents a different flake size distribution

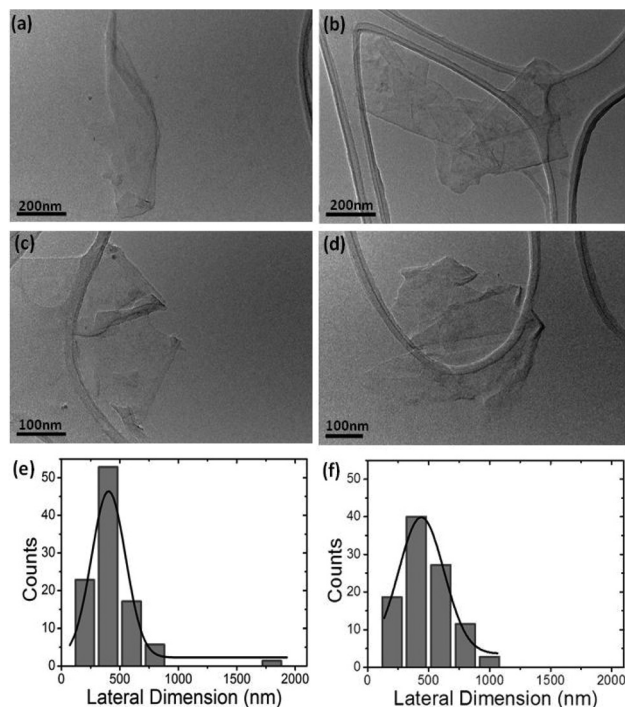


Fig. 8 (a, c) TEM images of stability of BMG powder in water after 2 hours and (b, d) 24 hours. Statistical lateral dimension Gaussian distribution from TEM images of BMG powder in water (e) after 2 hours and (f) 24 hours.

and a completely different C/O ratio (characterization data of GO in Fig. S3 and Table S1, ESI[†]). UV-Vis data reveal a different profile in GO but again 8 h as the inflection point (Fig. 7e). In light of these findings, we need to emphasize the importance of time when dealing not only with pristine GR, but also with its chemical derivatives. An experiment carried out in a few hours will not provide the same results compared to what is performed in a day or more. The structural characteristics of GR supplied to cells may not be the same, and therefore this should be taken into account when interpreting the results.

Conclusion

In summary, the study of the behavior of GR-based systems with well-known toxicity, reproducible toxicological profile in biological systems and easiness to be transferred to any medical or biomedical application is necessary for nanomedicine research. However, the production of aqueous suspensions of GR, in the absence of detergents, has not been possible, due to the intrinsic hydrophobicity of the GR layers. Our contribution describes the solution of a very important problem in graphene handling, namely, its storage in powder form and its easy dissolution in water and aqueous media. This is going eventually to pave the way towards the evaluation of graphene in biology and medicine, something that today is not allowed, due to the intrinsic high hydrophobicity of

graphene. We have shown that freeze-dried GR aqueous suspensions provide a fine powder, which can be easily reverted to aqueous media by mild sonication with no change in its structure. More interestingly, with an eye on biological applications, the lyophilized GR samples may be readily dispersed in CCM with similar results, in the presence or absence of serum and antibiotics. Stability studies revealed a concentration-independent partial sedimentation of GR materials, ending up in the loss of 25–30% of the initial concentration in only 2 h. In our experiments also the more hydrophilic GO derivative leaves sediments after 8 h which should be seriously taken into account in any biological experiments.

Experimental section

Materials

Solvents were purchased from SDS and Fluka. Chemicals were purchased from Sigma-Aldrich and used as received without further purification. Graphite was purchased from Bay Carbon, Inc. (SP-1 graphite powder, <http://www.baycarbon.com>) and used without purification. Ultrapure Milli-Q water ($\rho \leq 18 \text{ M}\Omega \text{ cm}^{-1}$) was used throughout. Commercially-sourced graphene oxide was prepared from powdered carbon fibres (GANF Helical-Ribbon Carbon Nanofibres) manufactured by the Grupo Antolin Ingenieria, GANF®.³³ The powder was dispersed in ultrapure water and the suspension was repeatedly filtered and rinsed with copious amounts of water to remove the presence of acids.

Cell culture media (CCM) were acquired from Sigma Aldrich. Two different media were tested: one with lower a glucose content (RPMI-1640, Ref. R8758), namely 2 g L^{-1} , and another one with higher glucose content (Dulbecco's Modified Eagle Medium, DMEM, Ref. D5796), *i.e.* 4.5 g L^{-1} . Both media were employed in order to cover a wide range of possible biological experiments thereof, which may need one or the other. The different composition of each medium can be checked from the seller's website (for RPMI, see <https://www.sigma-aldrich.com/content/dam/sigma-aldrich/docs/Sigma/Formulation/r8758for.pdf>; for DMEM, see <http://www.sigmaaldrich.com/content/dam/sigma-aldrich/docs/Sigma/Formulation/d5796for.pdf>). Fetal bovine serum (FBS) was acquired also from Sigma Aldrich (Ref. F0804) and the Gentamycin sulfate antibiotic was purchased from Lonza (Ref. BE02-012E, Lot# 2MB257), both used as received with no further treatment. The supplemented CCM was made by adding 10% (v/v) FBS and 1% (v/v) Gentamycin sulfate, and used freshly prepared.

Characterization techniques

The thermogravimetric analyses (TGA) were performed with a TGA Q50 (TA Instruments) at $10 \text{ }^\circ\text{C min}^{-1}$ under nitrogen flow, from $100 \text{ }^\circ\text{C}$ to $800 \text{ }^\circ\text{C}$.

X-Ray photoelectron spectra (XPS) were obtained with a VG Escalab 200R spectrometer equipped with a hemispherical electron analyser with a pass energy of 50 eV and a Mg K α ($h\nu = 1254.6 \text{ eV}$) X-ray source, powered at 120 W. The binding

energies were calibrated relative to the C 1s peak at 284.8 eV. High-resolution spectra envelopes were obtained by curve fitting synthetic peak components using the software "XPS peak". Symmetric Gaussian-Lorentzian curves were used to approximate the line shapes of the fitting components. Atomic ratios were computed from experimental intensity ratios and normalized by atomic sensitivity factors.

Elemental analysis (EA) was performed in a LECO CHNS-932 analyzer (Model No. 601-800-500).

Raman spectra were recorded with an InVia Renishaw microspectrometer equipped with 532 nm and 633 nm point-based lasers, respectively. In all cases power density was kept below $1 \text{ mW } \mu\text{m}^{-2}$ to avoid laser heating effects. Raman samples were prepared from stable diluted dispersions of graphene by drop-casting over silicon oxide surfaces (Si-Mat silicon wafers, CZ), and left to evaporate under ambient conditions. When CCM was used to disperse graphene, prior to Raman analysis (RPMI, as received), the sample deposited on the substratum was immersed for 3 seconds in hot water ($70 \text{ }^\circ\text{C}$) and dried at room temperature. The obtained spectra (after probing at least 50–60 random locations on each sample) were fitted with Lorentzian-shaped bands in their D, G and 2D peaks to ascertain band positions, widths and intensities.

Two-dimensional Raman mappings were performed with the 532 nm laser by using the line-based option (streamline). The whole set of spectra obtained was fitted under equal conditions and the band parameters were plotted in different colours.

For the TEM analyses, stable dispersions of graphene (the same used for Raman analysis) were diluted as necessary and dip-cast on Lacey copper grids (3.00 mm, 200 mesh), coated with carbon film, and dried under vacuum. The sample was investigated by using a High-Resolution Transmission Electron Microscope (HRTEM) JEOL 2100 at an accelerating voltage of 100 kV.

Preparation of graphene dispersions

The milling treatments were carried out in a Retsch PM100 planetary mill under an air atmosphere. Graphite (7.5 mg) and melamine (22.5 mg) were introduced in a stainless steel grinding bowl with 10 stainless steel balls (1 cm diameter each). The bowl was closed and placed within the planetary mill. The ball-milling treatment conditions were 100 rpm for 30 min under a static air atmosphere at room temperature. After the treatment, the resulting solid mixture was suspended in 20 mL of water and sonicated for 1 min. Melamine leftovers were washed away by inserting this liquid medium into a dialysis sack (Spectrum Labs, Ref. #132655, 6–8 kDa MWCO) and dialyzed against water at $70 \text{ }^\circ\text{C}$ with frequent replacements and mild sonication cycles until no melamine was detected in the washing water. Then, the resulting suspension was left to settle down for five days while some precipitate (mainly graphite and poorly exfoliated graphene) segregated from the liquid. The liquid fraction with stable sheets in suspension (few-layer graphene) was carefully extracted.

Freeze-drying of graphene aqueous dispersions

A given volume of aqueous graphene was placed in plastic containers and externally frozen with liquid nitrogen until the whole liquid became ice. Then, the container was sealed with aluminium foil, inserted into a Telstar Lyoquest device and lyophilized at $-80\text{ }^{\circ}\text{C}$ and a pressure of 0.005 bar, until obtaining the powder.

UV-Vis stability experiments

UV-Vis spectra were recorded in 1 cm quartz cuvettes on a Cary 5000 UV-vis-NIR spectrophotometer. Dual beam mode and baseline correction were used throughout the measurements to scan the maximum absorbance at 660 nm for BMG and 386 nm for graphene oxide (GO), for 2 hours and 24 hours at different time intervals. The maximum absorbance for GO was chosen on the basis of the wavelength in which the CCM (DMEM, with or without supplements) showed lower evolution of UV-Vis absorbance over time.

The concentration of graphene samples was determined from the optical absorption coefficient at maximum absorbance, using $A = \alpha \cdot l \cdot c$, where l (m) is the light path length, c (g L^{-1}) is the concentration of dispersed graphene material, and α ($\text{L g}^{-1} \text{m}^{-1}$) is the absorption coefficient, with $\alpha = 690 \text{ L g}^{-1} \text{m}^{-1}$ at 660 nm and $\alpha = 1130 \text{ L g}^{-1} \text{m}^{-1}$ at 386 nm for BMG and GO respectively. In both cases, the optical absorbance divided by cell length against the concentration exhibited Lambert–Beer behaviour.

Acknowledgements

We acknowledge financial support from the EU FP7-ICT-2013-FET-F GRAPHENE Flagship project (no. 604391), and from the Spanish Ministry of Economy and Competitiveness (MINECO) under project grant CTQ2014-53600-R. We thank Grupo Antolin for kindly supplying the graphene oxide material (<http://www.granph-acm.com/products>). Dr J. M. González-Domínguez greatly acknowledges MINECO for his researcher grant (Formación Postdoctoral).

Notes and references

- 1 A. C. Ferrari, F. Bonaccorso, V. Falco, K. S. Novoselov, S. Roche, P. Bøggild, S. Borini, F. Koppens, V. Palermo, N. Pugno, J. a. Garrido, R. Sordan, A. Bianco, L. Ballerini, M. Prato, E. Lidorikis, J. Kivioja, C. Marinelli, T. Ryhänen, A. Morpurgo, J. N. Coleman, V. Nicolosi, L. Colombo, A. Fert, M. Garcia-Hernandez, A. Bachtold, G. F. Schneider, F. Guinea, C. Dekker, M. Barbone, C. Galiotis, A. Grigorenko, G. Konstantatos, A. Kis, M. Katsnelson, C. W. J. Beenakker, L. Vandersypen, A. Loiseau, V. Morandi, D. Neumaier, E. Treossi, V. Pellegrini, M. Polini, A. Tredicucci, G. M. Williams, B. H. Hong, J. H. Ahn, J. M. Kim, H. Zirath, B. J. van Wees, H. van der Zant, L. Occhipinti, A. Di Matteo, I. a. Kinloch, T. Seyller, E. Quesnel, X. Feng, K. Teo, N. Rupesinghe, P. Hakonen, S. R. T. Neil, Q. Tannock, T. Löfwander and J. Kinaret, *Nanoscale*, 2014, **7**, 4598.
- 2 R. Ciriminna, N. Zhang, M.-Q. Yang, F. Meneguzzo, Y.-J. Xu and M. Pagliaro, *Chem. Commun.*, 2015, **51**, 7090.
- 3 K. E. Whitener and P. E. Sheehan, *Diamond Relat. Mater.*, 2014, **46**, 25.
- 4 M. Yi and Z. Shen, *J. Mater. Chem. A*, 2015, **3**, 11700.
- 5 J. N. Coleman, *Acc. Chem. Res.*, 2013, **46**, 14.
- 6 A. Ciesielski and P. Samori, *Chem. Soc. Rev.*, 2014, **43**, 381.
- 7 A. Bianco, *Angew. Chem., Int. Ed.*, 2013, **52**, 4997 (and references therein).
- 8 K. Yang, L. Feng, H. Hong, W. Cai and Z. Liu, *Nat. Protoc.*, 2013, **8**, 2392.
- 9 J. Kim, S. Kwon, D.-H. Cho, B. Kang, H. Kwon, Y. Kim, S. O. Park, G. Y. Jung, E. Shin, W.-G. Kim, H. Lee, G. H. Ryu, M. Choi, T. H. Kim, J. Oh, S. Park, S. K. Kwak, S. W. Yoon, D. Byun, Z. Lee and C. Lee, *Nat. Commun.*, 2015, **6**, 8294.
- 10 X. An, T. Simmons, R. Shah, C. Wolfe, K. M. Lewis, M. Washington, S. K. Nayak, S. Talapatra and S. Kar, *Nano Lett.*, 2010, **10**, 4295.
- 11 H. Yang, Y. Hernandez, A. Schlierf, A. Felten, A. Eckmann, S. Johal, P. Louette, J. J. Pireaux, X. Feng, K. Mullen, V. Palermo and C. Casiraghi, *Carbon*, 2013, **53**, 357.
- 12 F. Irin, M. J. Hansen, R. Bari, D. Parviz, S. D. Metzler, S. K. Bhattacharia and M. J. Green, *J. Colloid Interface Sci.*, 2015, **446**, 282.
- 13 M. Lotya, Y. Hernandez, P. J. King, R. J. Smith, V. Nicolosi, L. S. Karlsson, M. Blighe, S. De, Z. Wang, I. T. MCGovern, G. S. Duesberg, J. N. Coleman and F. M. Blighe, *J. Am. Chem. Soc.*, 2009, **131**, 3611.
- 14 M. Lotya, P. J. King, U. Khan, S. De and J. N. Coleman, *ACS Nano*, 2010, **4**, 3155.
- 15 M. C. Duch, G. R. S. Budinger, Y. T. Liang, S. Soberanes, D. Urich, S. E. Chiarella, L. a. Campochiaro, A. Gonzalez, N. S. Chandel, M. C. Hersam and G. M. Mutlu, *Nano Lett.*, 2011, **11**, 5201.
- 16 A. B. Bourlino, V. Georgakilas, R. Zboril, T. a. Steriotis, A. K. Stubos and C. Trapalis, *Solid State Commun.*, 2009, **149**, 2172.
- 17 S. Ahadian, M. Estili, V. J. Surya, J. Ramón-Azcón, X. Liang, H. Shiku, M. Ramalingam, T. Matsue, Y. Sakka, H. Bae, K. Nakajima, Y. Kawazoe and A. Khademhosseini, *Nanoscale*, 2015, **7**, 6436.
- 18 A. Pattammattel and C. V. Kumar, *Adv. Funct. Mater.*, 2015, **25**, 7088.
- 19 M. Creighton, I. Rangel, J. Mendez and J. Huang, *Small*, 2013, **9**, 1921.
- 20 V. León, M. Quintana, M. A. Herrero, J. L. G. Fierro, A. de la Hoz, M. Prato and E. Vázquez, *Chem. Commun.*, 2011, **47**, 10936.
- 21 V. León, A. M. Rodriguez, P. Prieto, M. Prato and E. Vázquez, *ACS Nano*, 2014, **8**, 563.
- 22 A. Servant, V. Leon, D. Jasim, L. Methven, P. Limousin, E. Vázquez, M. Prato and K. Kostarelos, *Adv. Healthcare Mater.*, 2014, **3**, 1334.

- 1 23 A. Fabbro, D. Scaini, V. Leon, E. Vázquez, G. Cellot, G. Privitera, L. Lombardi, F. Torrisi, F. Tomarchio, F. Bonaccorso, S. Bosi, A. C. Ferrari, L. Ballerini and M. Prato, *ACS Nano*, 2015, **10**, 615.
- 5 24 C. M. E. Gossner, J. Schlundt, P. Ben Embarek, S. Hird, D. Lo-Fo-Wong, J. J. O. Beltran, K. N. Teoh and A. Tritscher, *Environ. Health Perspect.*, 2009, **117**, 1803.
- 25 C. Neumann, S. Reichardt, P. Venezuela, M. Drögeler, L. Banszerus, M. Schmitz, K. Watanabe, T. Taniguchi, F. Mauri, B. Beschoten, S. V. Rotkin and C. Stampfer, *Nat. Commun.*, 2015, **6**, 8429.
- 10 26 U. Mogera, R. Dhanya, R. Pujar, C. Narayana and G. U. Kulkarni, *J. Phys. Chem. Lett.*, 2015, **6**, 4437.
- 15 27 A. C. Ferrari, J. C. Meyer, V. Scardaci, C. Casiraghi, M. Lazzeri, F. Mauri, S. Piscanec, D. Jiang, K. S. Novoselov, S. Roth and A. K. Geim, *Phys. Rev. Lett.*, 2006, **97**, 187401.
- 28 F. Torrisi, T. Hasan, W. Wu, Z. Sun, A. Lombardo, T. S. Kulmala, G.-W. Hsieh, S. Jung, F. Bonaccorso, P. J. Paul, D. Chu and A. C. Ferrari, *ACS Nano*, 2012, **6**, 2992.
- 5 29 A. C. Ferrari and J. Robertson, *Phys. Rev. B: Condens. Matter*, 2000, **61**, 14095.
- 30 A. C. Ferrari and J. Robertson, *Phys. Rev. B: Condens. Matter*, 2001, **64**, 075414.
- 10 31 T. L. Moore, L. Rodriguez-Lorenzo, V. Hirsch, S. Balog, D. Urban, C. Jud, B. Rothen-Rutishauser, M. Lattuada and A. Petri-Fink, *Chem. Soc. Rev.*, 2015, **44**, 6287.
- 15 32 W. Hu, C. Peng, M. Lv, X. Li, Y. Zhang, N. Chen, C. Fan and Q. Huang, *ACS Nano*, 2011, **5**, 3693.
- 33 H. Varela-Rizo, I. Rodriguez-Pastor, C. Merino and I. Martin-Gullón, *Carbon*, 2010, **48**, 3640.

20 20

25 25

30 30

35 35

40 40

45 45

50 50

55 55